Performant on-chip photonic detectors with lateral p-i-n silicon-germanium heterojunctions

Daniel Benedikovic, Léopold Virot, Guy Aubin, Jean-Michel Hartmann, Farah Amar, Xavier Le Roux, Carlos Alonso-Ramos, Eric Cassan, Delphine Marris-Morini, Frederic Boeuf, et al.

Performant on-chip photonic photodetectors with lateral p-i-n silicon-germanium heterojunctions (invited presentation)

Daniel Benedikovic*[,a], Leopold Virot[b], Guy Aubin[a], Jean-Michel Hartmann[b], Farah Amar[a], Xavier Le Roux[a], Carlos Alonso-Ramos[a], Eric Cassan[a], Delphine Marris-Morini[a], Frederic Boeuf[c], and Laurent Vivien[a]

[a]Université Paris-Saclay, CNRS, Centre de Nanosciences et de Nanotechnologies, 91120 Palaiseau, France
[b]University Grenoble Alpes and CEA, LETI, Minatec Campus, F-38054 Grenoble, France
[c]Technology R&D, STMicroelectronics SAS, 850 Rue Jean Monnet, 38920 Crolles, France

ABSTRACT

Short-distance optical communications and large-scale networks are central in telecom, datacom, and information processing technologies. Such applications require high transmission capacity, low energy consumption, implementation at the chip-scale level and cost-effective production. Silicon photonics (SiP) is well-positioned to tackle these growing needs. Indeed, photonic chips enable dense integration of complex functions through light-driven, compact, and high-performance devices. SiP is boosted by complementary metal-oxide-semiconductor (CMOS) processes and toolsets used for decades in the microelectronic industry. CMOS-friendly manufacturing, mature germanium (Ge) epitaxy and open-access foundry model are advantageous for monolithic integration, where a low-loss silicon (Si) platform meets advanced opto-electrical efficiency and fast response time. Optical photodetectors are key building blocks in the SiP library. They leverage progresses made in design strategies, material processing and seamless Si CMOS integration. In particular, chip-integrated silicon-germanium (Si-Ge) photodetectors are aiming for fast, sensitive, and energy-aware operation, with performances that are becoming competitive or even superior to existing and well-adopted III/V-based counterparts. In this work, we present our recent advances in waveguide-integrated p-i-n photodetectors based on double silicon-germanium-silicon (Si-Ge-Si) heterojunctions. Hetero-structured Si-Ge-Si photodetectors with a butt-waveguide-coupling and a lateral p-i-n electrical junction are most promising to detect light on a silicon chip at near-infrared (near-IR) wavelengths. They rely on unique integration approach that yields structures with compact footprints and properly

engineered waveguide geometries. Such devices then benefit from improved modal confinement and overall control over the intrinsic region. They are also easy to fabricate and integrate with other passive and active components on a single chip. Si-Ge-Si p-i-n photodetectors were fabricated on 200 mm silicon-on-insulator (SOI) substrates using industrial-scale semiconductor manufacturing processes. Fabricated p-i-n structures were operated under low-voltages and in avalanche regime, respectively. In both situations, devices showed up a reliable high-speed, low-noise, and sensitive signal detection within a mainstream telecom waveband around 1.55 μm.

Keywords: Optical photodetectors, Silicon photonics, Silicon-on-insulator, Germanium, PIN photodiode, Avalanche photodiode, Complementary metal-oxide-semiconductor technology, optical communications, energy consumption

1. INTRODUCTION

Advanced technologies for photonic integration become key enablers to realize optical chips and afford access towards many emerging applications. Surging applications range from sensing, biomedicine and health sciences through object recognition, LIDAR and civil engineering up to optical communications and interconnects, to name a few. In particular, optical communications and optical interconnects are essential drivers in the field of photonics integration. Both application domains replace traditional, yet inferior in performance, metalized electrical wirings in a variety of chip-scale links. In this context, photonic technologies are particularly promising for long-haul optical fiber systems as well as short-reach data centers, which may include clouds and storages or high performance computing, among others rising areas. Dense integration of photonic components on a single semiconductor chip is a natural route to tackle challenges associated with cost, speed and bandwidth as well as energy consumption [1-4].

Compact and high-performance components are now available through photonic integration in a single chip, leveraging monolithic integration approach [4,5]. This can be achieved thanks to two group-IV materials: silicon (Si) and germanium (Ge). Group-IV semiconductor chips are thus very perspective as they can deliver complex on-chip functions [5-10], ranging from light generation and modulation through light processing, and up to light detection. Si is an indirect bandgap material with an energy of 1.14 eV, while Ge has a quasi-direct energy bandgap, carrying an energy of 0.67 eV. Using Ge then offers great advantages and desired complementarities compared to pure Si platforms.

Optical photodetectors are components that transform optical signals into electrical signals. Optical photodetectors that are based upon group-IV materials and silicon-on-insulator (SOI) waveguide system attracted a large attention. Such photodetectors can be fabricated using mainstream Si-foundry processes and procedures, providing accurate reproducibility and high yields. In addition, compatibility with complementary metal-oxide-semiconductor (CMOS) technology opens up a way for a mass-scale development with a reduced processing and production expenses [11-29]. Alternatively, III-V-based photodetectors implemented on SOI substrates are good candidates. They can be realized through hybrid or heterogeneous integration with chip-to-chip bonding or direct hetero-epitaxial growth [30,31]. However, hybrid or heterogeneous integration bring additional drawbacks into the overall process flow, including manufacturing complexity and associated higher production costs. This way, utilization of group-IV semiconductors is foreseen to be optimal for the feasible monolithic chip integration.

Different kinds of waveguide-integrated p-i-n photodetectors have been investigated in the last years, usually taking the form of full-Ge structures [12-22] and combined Si-Ge devices [23-29]. Homo- and hetero-junction optical photodetectors use p-i-n junctions. The opto-electrical performance of homo-junction detectors is typically affected by process issues (ion implantation for p- and n-doped regions and metal vias are performed in/on top of Ge) and optical factors (weak modal field confinement within the intrinsic device zone). Consequently, their opto-electrical performance outputs are not as high as their hetero-junction counterparts. Full-Ge p-i-n's have higher dark currents, lower bandwidths, and reduced responsivity [12-22]. In opposite, hetero-structured Si-Ge photodetectors take advantages of improved fabrication processes [23-29] and better optical confinements within the intrinsic (light-absorbing) region. Hetero-structured photodetectors are fabricated with full-Si metal via-contacts and doping. Both aspects help to improve the device performances. However, conventional p-i-n structures have limited responsivity up to 1.24 A/W at 1.55 μm. Moreover, their optical power sensitivity for high-speed modulated signals is modest as well. Moreover, simple p-i-n devices also generate low electrical outputs, and thus extra amplification stages with additional electronic components need to be employed.

Better performances can be expected by using photodetectors with an internal multiplication gain [32-45], so-called avalanche photodetectors (APDs). APDs can be found as metal-semiconductor-metal (MSM), p-i-n or separate absorption charge multiplication (SACM) structures. MSM devices can be driven at low voltages, with CMOS-compliant fabrication. On the other hand, they exhibit high dark currents and limited sensitivity [32] . In contrast, SACM photodetectors capitalize on a low multiplication noise of Si within the multiplication region [33,34,38,39,42-46].

However, SACM devices require excessively high voltages and still operate with moderate speeds. Even though recent SACM photodetectors can provide higher operation for conventional on-off keying (OOK) modulation or multi-level pulse amplitude modulation (PAM) formats, they are still realized with additional amplification components such as trans-impedance amplifiers (TIAs) and limiting amplifiers (LAs), which however, affect their energy consumption [43,44].

In this work, we present recent advances in the development of p-i-n photodetectors with lateral silicon-germanium-silicon (Si-Ge-Si) heterojunctions. Si-Ge hetero-structured photodetectors were fabricated on top of 200-mm SOIs using Si-foundry processes. P-i-n photodetectors that are operated at low reverse voltages yielded low dark-currents (~100 nA), photodiode bandwidth exceeding 50 GHz, and high photo-responsivities, approaching a level of 1.2 A/W as well as allowing high-speed 40 Gbps operation. P-i-n waveguide-integrated photodetectors with lateral heterojunctions operated in an avalanche regime offer additional performance improvements. High-speed and low-noise characteristics were obtained with a gain-bandwidth product of about 210 GHz and a low excess noise with a carrier impact ionization ratio of ~0.25. Measured sensitivity was -11 dBm for a conventional OOK modulation at 40 Gbps transmission bit rate, considering an error rate level of 10^{-9}.

The manuscript is organized in the following way. After the introduction in *Section 1*, *Section 2* reports on a low-bias operation of waveguide-integrated Si-Ge-Si p-i-n

photodetectors, while *Section 3* sums up recent achievements for avalanche-mode-operated Si-Ge-Si p-i-n photodetectors. Finally, conclusions are drawn in *Section 4*.

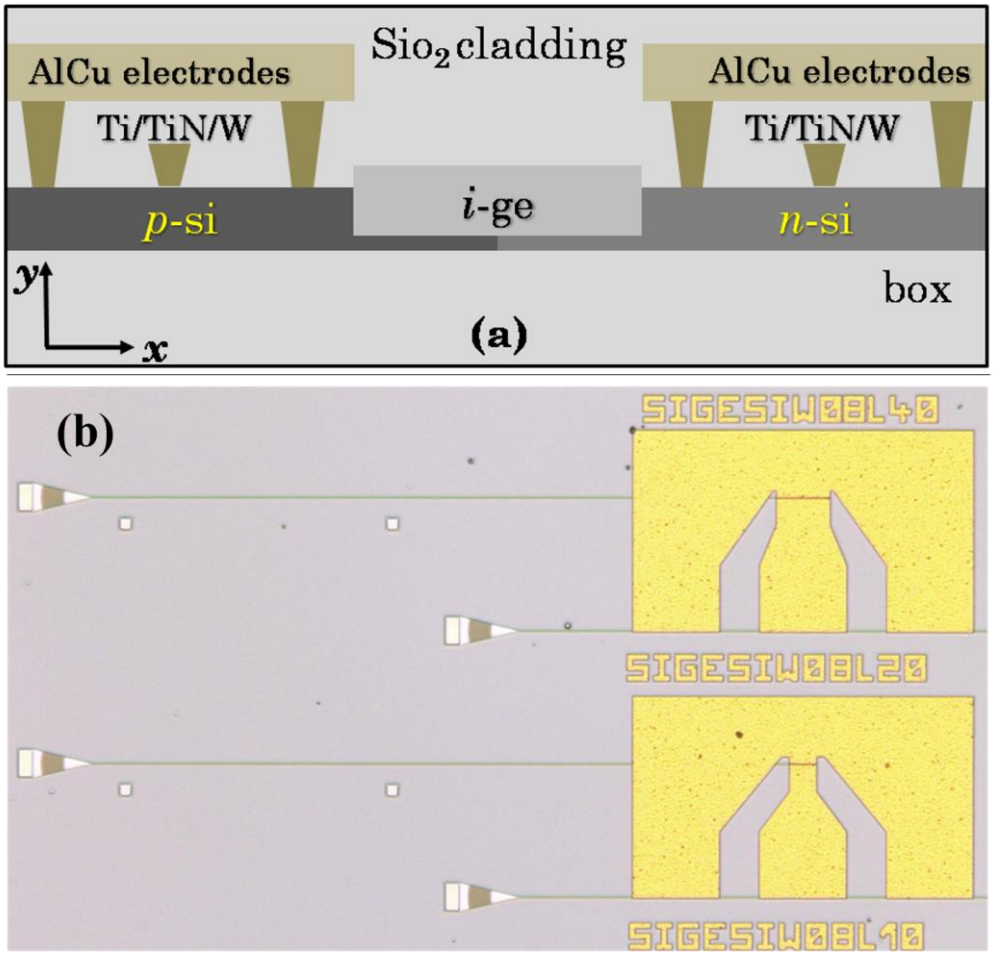

Figure 1. (a) Cross-sectional schematics (x-y plane) of the waveguide-integrated photodetector with a lateral silicon-germanium-silicon heterojunction. (b) Optical micrograph image of a few fabricated hetero-structured p-i-n photodetectors.

Optical photodetectors with lateral Si-Ge-Si hetero-junctions are shown schematically in Fig. 1a (a cross-sectional schematics), while in Fig. 1b., we can found an optical microscopy image of fabricated hetero-structured photodetectors. Here, optical photodetectors are implemented with SOI waveguides. A low-loss butt-waveguide-coupling is combined with laterally arranged electrical p-i-n junctions. Top Si layer of 220 nm is positioned on top of 2 μm thick buried oxides (BOXs). This integration approach helps to fabricate compact Ge photodetectors at the end of Si waveguides with good quality. The Ge film (i.e. the intrinsic photodetector region) is ~260 nm thick. This light-absorbing layer is selectively grown in narrow Si trenches, deeply etched at the

end of waveguides. The remaining Si thickness at the bottom of those trenches is about 60 nm. Ge is sandwiched between heavily doped Si slabs, having metal contacts formed on top. Variations in widths and lengths of the intrinsic device region are included on the mask. Off-chip coupling is realized via surface grating couplers. They inject the input light from an optical fiber into the Si waveguides, followed by hetero-structured p-i-n photodetectors. Surface grating couplers and Si interconnecting waveguides are optimized for transverse electric (TE) polarization at 1.55 μm. The injection Si waveguides are single-mode, with a cross-section of 220 nm by 500 nm (thickness by width) [27,28].

Optical photodetectors were fabricated using CMOS-friendly tools in cleanroom facilitates of CEA LETI. They were realized on 200 mm SOI substrates. The fabricated devices were fully characterized using static current-voltage measurements, small-signal radio-frequency testing, and large-signal data link measurements for eye diagram acquisitions and bit-error-rate assessments. More details about the fabrication and characterization can be found in Refs [27-29,40,41].

2. P-I-N DIODE OPERATION

Dark-current curves of different devices are shown in Fig. 2a. Dark-currents under 1 V bias remain consistently low (< 1 μA), typically of the order of a few tens of nA. The largest dark-current levels of around 150 nA are measured for the largest devices (1 μm wide and 40 μm long). The dark-current rises up with the operating voltage (for a fixed device geometry). Compact photodiodes are required as they facilitate low noise operation. Typically, p-i-n devices driven at low voltages need to have additional amplification stages with TIAs and LAs due to lower electrical outputs.

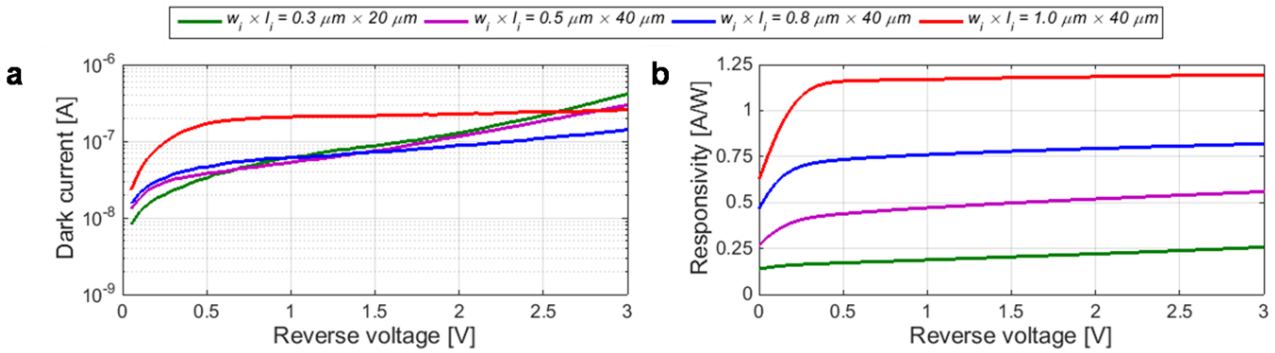

Figure 2. (a) Dark-current and (b) photo-responsivity as a function of reverse voltage for different geometries of hetero-structured silicon-germanium-silicon photodetectors.

Figure 2b shows the diode photo-responsivity as a function of reverse voltages, measured at a reference laser emission wavelength of 1.55 μm. Photo-responsivity is

determined from the current-voltage measurements with a light coupled into the photodetector. As we can see, wider and longer devices yield higher levels of photo-responsivity. Under 0 V, the responsivity of hetero-structured Si-Ge-Si photodetectors is always low. In this case, the built-in electric field is the weak. The smallest devices (0.3 μm wide and 20 μm long) have responsivity of 0.14 A/W The largest photodetectors (1 μm wide and 40 μm long) have responsivity of 0.63 A/W. It is evident that the responsivity increases with the voltage. This is a consequence of a higher electric field inside the intrinsic Ge region. The measured device responsivities at -0.5 V are: 0.17 A/W, 0.44 A/W, 0.73 A/W and 1.16 A/W, respectively. Corresponding quantum efficiencies, at 0.5 V bias and an illumination wavelength of 1.55 μm, are estimated to be 13.8%, 35.1%, 58.7% and 92.8% for the same group of devices.

The bandwidth of hetero-structured photodetectors was studied via small-signal radio-frequency (RF) measurements. Normalized S21 traces for different p-i-n geometriess and different operating voltages (0 V and 1 V) are shown in Fig. 3. Zero-bias operation, depicted in Fig. 3a, yields low cut-off frequencies of 4.8 GHz, 3.8 GHz, 1.3 GHz, and 1.1 GHz for particular device layouts. This small values are attributed to the long transit time of carriers and the weak built-in electric field within the intrinsic device region. These observations are in good coincidence with a low photo-responsivities measured under such operating conditions. In opposition, hetero-structured p-i-n biased at 1 V yielded much better bandwidths. We measured 35 GHz, 24.2 GHz, 15.7 GHz, and 6.7 GHz for the same geometers (see Fig. 3b). The improved bandwidth is also in line with the improvement observed in diode photo-responsivities.

A summary of 3 dB down bandwidth as a function of operating reverse voltages for all tested hetero-structured p-i-n photodetectors is shown in Fig. 3c. As we can see, photodetectors with narrower hetero-junction regions yielded much faster frequency responses. In particular, frequency response well beyond 50 GHz for a 2 V bias point was measured for the 0.3 μm wide photodetectors. It is otherwise obvious that the 3 dB bandwidth increases as the width of the intrinsic Ge region decreases. Moreover, we also observed that for a fixed width of the intrinsic photodetector region, the extracted cut-off frequencies do not really depend on the length of the intrinsic Ge region. This may indicate that the frequency response of the hetero-structured Si-Ge-Si p-i-n photodetectors is not mainly limited by the product between the diode resistance and the diode capacitance, i.e. resistance-capacitance (RC) delay. The main bandwidth (and speed) limitation for the hetero-structured p-i-n photodetectors comes from the carrier transit time.

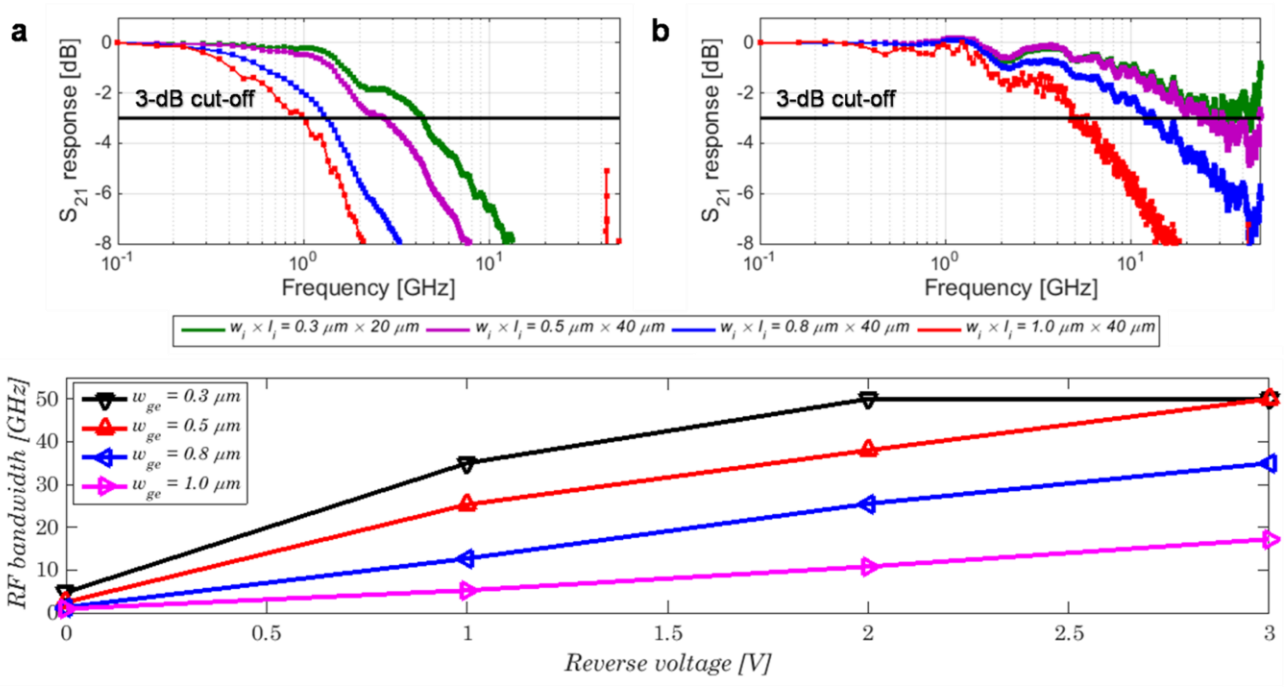

Figure 3. Normalized S_{21} parameters as a function of the radio-frequency for different silicon-germanium-silicon photodetector geometries and different operating reverse bias conditions: (a) 0 V and (b) 1 V. (c) Opto-electrical bandwidths versus reverse bias voltage for different widths of the hetero-structured silicon-germanium-silicon photodetectors.

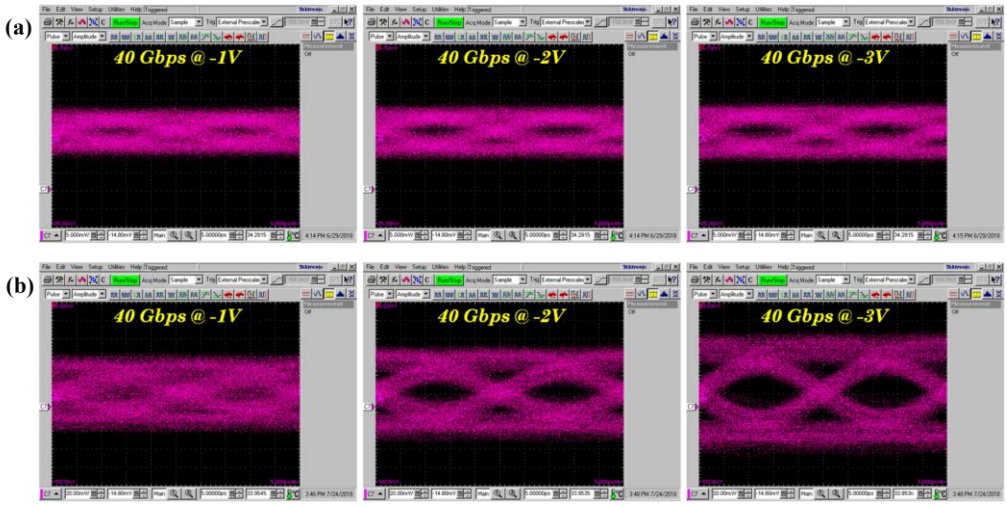

Figure 4. Evolution of electrical eye diagrams under low-reverse-voltage operation, considering a transmission bit rate of 40 Gbps. In-plane dimensions of hetero-structured silicon-germanium-silicon photodetectors are: (a) w_{ge} = 0.5 µm and l_{ge} = 40 µm and (b) w_{ge} = 1.0 µm and l_{ge} = 40 µm.

The high-speed operation of hetero-structured Si-Ge-Si pin photodetectors was further confirmed using large-signal data detection measurements. This was performed via eye-diagram acquisitions. The measured eye diagram apertures under different low-reverse-voltage operating conditions and a fixed transmission bit rate of 40 Gbps is shown in Fig. 4. Large-signal data assessments were carried out on hetero-structured p-i-n photodetectors with a 40-μm-long and 0.5- and 1.0-μm-wide Ge regions.

As can be seen in Fig. 4, opened eye diagram apertures suggest that high-speed signal detection up to 40 Gbps is readily achieved in all studied arrangements of hetero-structured p-i-n photodetectors. The limited opto-electrical bandwidth of the hetero-structured Si-Ge-Si photodetectors at 1V reverse voltages explains why retrieved electrical eye diagrams are starting to close. This effect is more obvious for devices with a wider intrinsic Ge region (1 μm wide and 40 μm long), shown in Fig. 4b. These trends are in a good agreement with the small-signal radio-frequency tests. Nevertheless, it is worth mentioning that the voltage control possibility preserves a superior high-data-rate detection capability, thus still enabling a device operation under low-voltages.

3. AVALANCHE DIODE OPERATION

The performance of hetero-structured p-i-n photodetectors can be further enhanced by operating the diode in the avalanche mode. We exploit an avalanche operation on a diode with 0.5 μm wide and 40 μm long intrinsic Ge region.

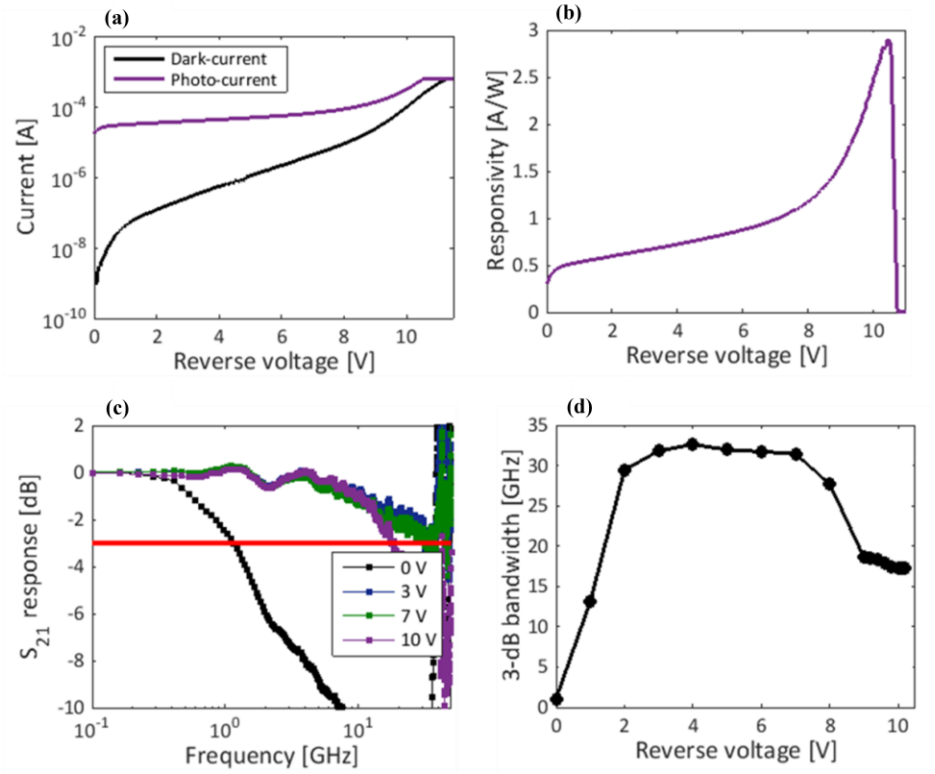

Figure 5. (a) Current-voltage (undr dark and light-illuminated states) and (b) responsivity-voltage curves of hetero-structured p-i-n photodetector. The wavelength of laser emission was 1.55 um, while the power coupled into the device was -12 dBm. (c) Normalized S21 response versus the radio-frequency of hetero-structured p-i-n photodetector, considering different operating reverse bias conditions. (d) 3-dB bandwidth as a function of reverse voltages.

Figure 5 shows opto-electrical performance obtained with avalanche-mode-operated hetero-structured p-i-n photodetectors. Figures 5a and 5b depict current- and responsivity-voltage curves of Si-Ge-Si p-i-n photodetector. In particular, Fig. 5a shows dark- and photo-currents as a function of an applied reverse voltage. As expected, the dark current rises up with the reverse bias, being a sign of operation in avalanche regime. At -1V, the dark-current is low (of about 50 nA). The avalanche breakdown is reached at a voltage of 11 V. The dark-current at an avalanche breakdown is 600 μA. The photo-current was generated from a laser source at a wavelength of 1.550 μm, with a launched power of about -12 dBm. The diode responsivity as a function of a reverse voltage is shown in Fig. 5b. The responsivity at 0 V and -1V are 0.3 A/W and 0.5 A/W. The device photo-responsivity increases further, reaching a peak near the avalanche breakdown. This peak value is 2.9 A/W, which corresponds to the avalanche multiplication gain of 5.8.

Figures 5c and 5d depict the 3 dB bandwidth characteristics properties of a 0.5 µm wide and 40 µm long hetero-structured Si-Ge-Si photodetector, operating in an avalanche regime. The measurements were performed at a reference wavelength of 1.550 µm, with an optical input power of about -18 dBm. Figure 5c shows four normalized S21 responses as a function of the radio frequency for different reverse voltages. Those reverse voltages are 0 V, 3 V, 7 V, and 10 V. Figure 5d summarizes the 3 dB down bandwidth. The 3 dB bandwidth increases from 1.2 up to 33 GHz as the voltage increases from 0 V up to 3 V. Then, the 3 dB bandwidth stays almost same in a range from 3 V up to 7 V. In this region, the photo-carriers reached their saturation velocity. Beyond a 7 V reverse voltage, the 3 dB down bandwidth reduces substantially due to the avalanche built-up time. At -10V (just below the avalanche breakdown), the diode bandwidth is still larger than 17 GHz. A maximum gain-bandwidth product up to 210 GHz was then obtained.

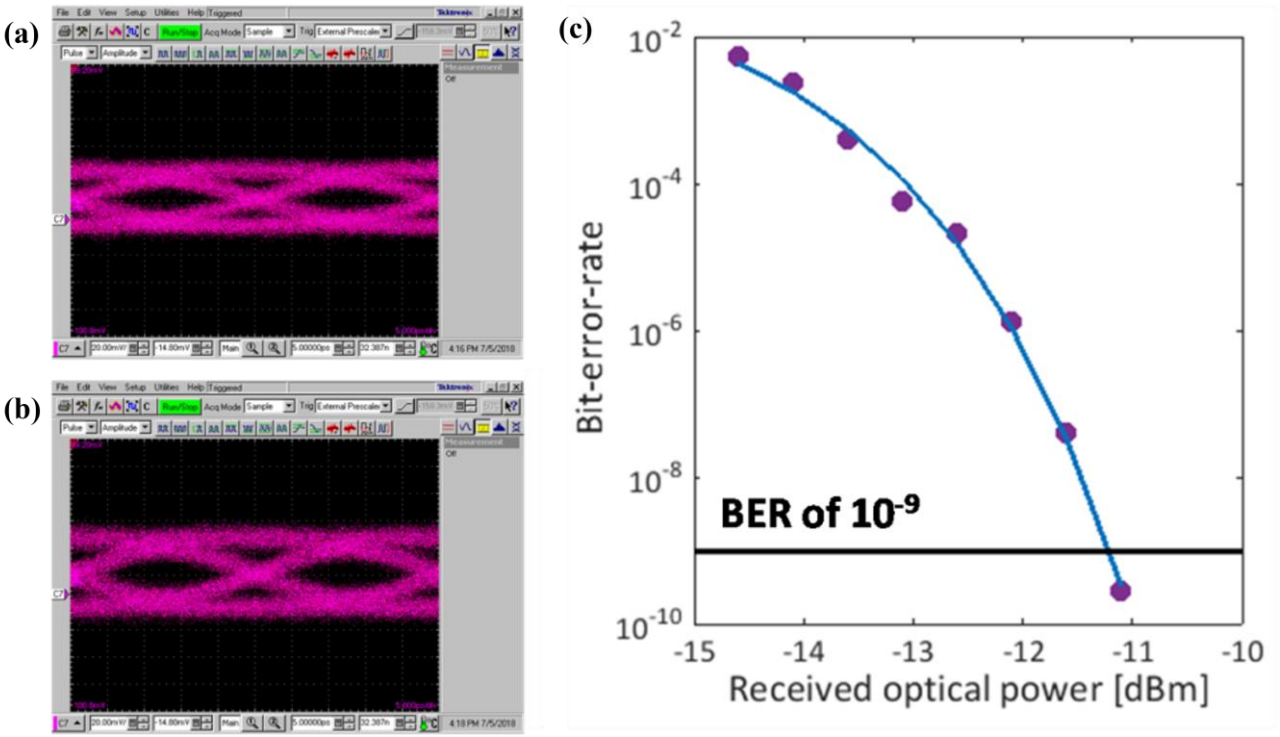

Figure 6. Electrical eye diagram apertures of 0.5 µm wide and 40 µm long hetero-structured p-i-n photodetector operating at 40 Gbps and different avalanche conditions: (a) -15 dBm and -7 V and (d) -15 dBm, and -10 V, respectively. (e) Bit-error-rate versus received optical power. Hetero-structured photodetector operates at 40 Gbps with a reverse voltage of 10 V.

The p-i-n avalanche photodetectors were also characterized via large-signal measurements using both eye diagram inspection and bit-error-rate (BER) assessments.

Figures 6a and 6b show the evolution of eye diagram apertures for an optical power level of -15 dBm and two different reverse voltages of 7 V and 10 V. The transmission bit rate was fixed in both cases to 40 Gbps. Figure 6c shows BER as a function of the received optical power. BER measurements were also performed for a 40 Gbps optical signals. The diode was biased at -10V. The measured optical power sensitivity, at a 10-9 BER level, is equal to -11 dBm.

4. CONCLUSION

We demonstrated our recent results on optical photodetectors based on lateral Si-Ge-Si p-i-n hetero-junctions. Such photodetectors take advantages from easy-to-implement integration approach that advantageously combine the butt-waveguide coupling and lateral hetero-structured junctions. In turn, this enables a device fabrication using well-developed Si-foundry processes. This integration techniques then results in lower fabrication complexity and better device performances. More specifically, p-i-n photodetectors operated at low voltages exhibited low dark-currents (~150 nA), cut-off frequencies beyond 50 GHz, and photo-responsivities of 1.2 A/W. Hetero-structured p-i-n photodetectors also enabled a high-speed operation up to 40 Gbps at low biases. Moreover, p-i-n photodetectors with lateral heterojunctions operated in an avalanche regime offer additional performance improvements, especially providing enhanced signal quality and high-speed detection at the telecom waveband. High gain-bandwidth product of 210 GHz was obtained, enabling an error-free signal detection at a transmission bit rate of 40 Gbps, with a power sensitivity of -11 dBm for a 10-9 bit-error-rate. These demonstrations are promising for the deployment of high-speed, energy-aware, and low-cost photodetectors in future optical interconnects.

REFERENCES

[1] A. Alduino and M. Paniccia, “Wiring electronics with light,” Nature Photonics 1, 153-155 (2007).

[2] M. Asghari and A. V. Krishnamoorthy, “Energy-efficient communication,” Nature Photonics 5, 268-270 (2011).

[3] A. H. Atabaki, S. Moazeni, F. Pavanello, H. Gevorgyan, J. Notaros, L. Alloatti, M. T. Wade, C. Sun, S. A. Kruger, H. Meng, K. Al Qubaisi, I. Wang, B. Zhang, A. Khilo, C. V. Baiocco, M. A. Popović, V. M. Stojanović, and R. J. Ram, “Integrating photonics with silicon nanoelectronics for the next generation of systems on a chip,” Nature 556, 349-354 (2018).

[4] C. Sun, M. T. Wade, Y. Lee, J. S. Orcutt, L. Alloatti, M. S. Georgas, A. S. Waterman, J. M. Shainline, R. R. Avizienis, S. Lin, B. R. Moss, R. Kumar, F. Pavanello, A. H. Atabaki, H. M. Cook, A. J. Ou, Jo. C. Leu, Y.-H. Chen, K. Asanović, R. J. Ram, M. A. Popović, and V. M. Stojanović, "Single-chip microprocessor that communicates directly using light," Nature 528, 534-538 (2015).

[5] D. Thomson, A. Zilkie, J. E. Bowers, T. Komljenovic, G. T. Reed, L. Vivien, D. Marris-Morini, E. Cassan, L. Virot, J.-M. Fédéli, J.-M. Hartmann, J. H. Schmid, D.-X. Xu, F. Boeuf, P. O'Brien, G. Z. Mashanovich, and M. Nedeljkovic, "Roadmap on silicon photonics," Journal of Optics 18, 073003 (2016).

[6] R. Halir, A. Ortega-Moñux, D. Benedikovic, G. Z. Mashanovich, J. G. Wangüemert-Pérez, J. H. Schmid, Í. Molina-Fernández, and P. Cheben, "Subwavelength-Grating Metamaterial Structures for Silicon Photonic Devices," Proceedings of the IEEE 106, 2144-2157 (2018).

[7] D. Marris-Morini, V. Vakarin, J. M. Ramirez, Q. Liu, A. Ballabio, J. Frigerio, M. Montesinos, C. Alonso-Ramos, X. Le Roux, S. Serna, D. Benedikovic, D. Chrastina, L. Vivien, and G. Isella, "Germanium-based integrated photonics from near- to mid-infrared applications," Nanophotonics 7, 1781-1793 (2018).

[8] S. Wirths, R. Geiger, N. von den Driesch, G. Mussler, T. Stoica, S. Mantl, Z. Ikonic, M. Luysberg, S. Chiussi, J. M. Hartmann, H. Sigg, J. Faist, D. Buca, and D. Grutzmacher, "Lasing in direct-bandgap GeSn alloy grown on Si," Nature Photonics 9, 88-92, (2015).

[9] M. Berciano, G. Marcaud, P. Damas, X. Le Roux, P. Crozat, C. Alonso Ramos, D. Pérez Galacho, D. Benedikovic, D. Marris-Morini, E. Cassan, and L. Vivien, "Fast linear electro-optic effect in a centrosymmetric semiconductor ," Communications Physics 1, Article number 64, 1-9 (2018).

[10] D. Benedikovic, L. Virot, G. Aubin, J.-M. Hartmann, F. Amar, X. Le Roux, C. Alonso-Ramos, É. Cassan, D. Marris-Morini, J.-M. Fédéli, F. Boeuf, B. Szelag and L. Vivien, "Silicon–germanium receivers for short-wave-infrared optoelectronics and communications," Nanophotonics 10, 1059-1079, (2021).

[11] J. Michel, J. Liu, and L. C. Kimerling, "High-performance Ge-on-Si photodetectors," Nature Photonics 4, 527-534, (2010).

[12] L. Colace, G. Masini, G. Assanto, H.-C. Luan, K. Wada, and L. C. Kimerling, "Efficient high-speed near-infrared Ge photodetectors integrated on Si substrates," Applied Physics Letters 76, 1231-1233, (2000).

[13] T. Yin, R. Cohen, M. M. Morse, G. Sarid, Y. Chetrit, D. Rubin, and M. J. Paniccia, "31 GHz Ge n-i-p waveguide photodetectors on Silicon-on-Insulator substrate," Optics Express 15, 13965-13971, (2007).

[14] L. Colace, P. Ferrara, G. Assanto, D. Fulgoni, and L. Nash, "Low dark-current germanium-on-silicon near infrared detectors," IEEE Photonics Technology Letters 19, 1813-1842, (2007).
[15] D. Ahn, C.-Y. Hong, J. Liu, W. Giziewicz, M. Beals, L. C. Kimerling, J. Michel, J. Chen, and F. X. Kärtner, "High performance, waveguide integrated Ge photodetectors," Optics Express 15, 3916-3921, (2007).
[16] L. Vivien, M. Rouvière, J.-M. Fédéli, D. Marris-Morini, J.-F. Damlencourt, J.Mangeney, P. Crozat, L. El Melhaoui, E. Cassan, X. Le Roux, D. Pascal, and S. Laval, "High speed and high responsivity germanium photodetector integrated in silicon-on-insulator microwaveguide," Optics Express 15, 9843-9848, (2007).
[17] L. Vivien, J. Osmond, J.-M. Fédéli, D. Marris-Morini, P. Crozat, J.-F. Damlencourt, E. Cassan, Y. Lecunff, and S. Laval, "42 GHz p.i.n Germanium photodetector integrated in a silicon-on-insulator waveguide," Optics Express 17, 6252-6257, (2009).
[18] S. Assefa, F. Xia, S. W. Bedell, Y. Zhang, T. Topuria, P. M. Rice, and Y. A. Vlasov, "CMOS-integarted high-speed MSM germanium waveguide photodetector," Optics Express 18, 4986-4999, (2010).
[19] C. T. DeRoose, D. C. Trotter, W. A. Zortman, A. L. Starbuck, M. Fisher, M. R. Watts, and P. S. Davids, "Ultra compact 45 GHz CMOS compatible Germanium waveguide photodiode with low dark current," Optics Express 19, 24897-24904, (2011).
[20] L. Vivien, A. Polzer, D. Marris-Morini, J. Osmond, J. M. Hartmann, P. Crozat, E. Cassan, C. Kopp, H. Zimmermann, and J. M. Fédéli,, "Zero-bias 40Gbit/s germanium waveguide photodetector on silicon," Optics Express 20, 1096-1101, (2012).
[21] G. Li, Y. Luo, X. Zheng, G. Masini, A. Mekis, S. Sahni, H. Thacker, J. Yao, I. Shubin, K. Raj, J. E. Cunningham, and A. V. Krishnamoorthy, "Improving CMOS-compatible Germanium photodetectors," Optics Express 20, 26345-26350, (2012).
[22] H. Pan, S. Assefa, W. M. J. Green, D. M. Kuchta, C. L. Schow, A. V. Rylyakov, B. G. Lee, C. W. Baks, S. M. Shank, and Y. A. Vlasov, "High-speed receiver based on waveguide germanium photodetector wire-bonded to 90nm SOI CMOS amplifier," Optics Express 20, 18145-18155, (2012).
[23] Y. Zhang, S. Yang, Y. Yang, M. Gould, N. Ophir, A. E.-J. Lim, G.-Q. Lo, P. Magill, K. Bergman, T. Baehr-Jones, and M. Hochberg, "A high-responsivity photodetector absent metal-germanium direct contact," Optics Express 22, 11367-11375, (2014).

[24] S. Lischke, D. Knoll, C. Mai, L. Zimmermann, A. Peczek, M. Kroh, A. Trusch, E. Krune, K. Voigt, and A. Mai, “High bandwidth, high responsivity waveguide-coupled germanium p-i-n photodiode,” Optics Express 23, 27213-27220, (2015).
[25] H. T. Chen, P. Verheyen, P. De Heyn, G. Lepage, J. De Coster, P. Absil, G. Roelkens, and J. Van Campenhout, “High-Responsivity Low-Voltage 28-Gb/s Ge p-i-in Photodetector With Silicon Contacts,” IEEE Journal of Lightwave Technology 33, 820-824, (2015).
[26] H. Chen, P. Verheyen, P. De Heyn, G. Lepage, J. De Coster, S. Balakrishnan, P. Absil, W. Yao, L. Shen, G. Roelkens, and J. Van Campenhout, “-1 V 67 GHz bandwidth Si-contacted germanium waveguide p-i-n photodetector for optical links at 56 Gbps and beyond,” Optics Express 24, 4622-4631, (2016).
[27] L. Virot, D. Benedikovic, B. Szelag, C. Alonso-Ramos, B. Karakus, J.-M. Hartmann, X. Le Roux, P. Crozat, E. Cassan, D. Marris-Morini, C. Baudot, F. Boeuf, J.-M. Fédéli, C. Kopp, and L. Vivien, “Integrated waveguide PIN photodiodes exploiting lateral Si/Ge/Si heterojunction,” Optics Express 25, 19487-19496, (2017).
[28] D. Benedikovic, L. Virot, G. Aubin, F. Amar, B. Szelag, B. Karakus, J.-M. Hartmann, C. Alonso-Ramos, X. Le Roux, P. Crozat, E. Cassan, D. Marris-Morini, C. Baudot, F. Boeuf, J.-M. Fédéli, C. Kopp, and L. Vivien, “25 Gbps low-voltage hetero-structured silicon-germanium waveguide pin photodetectors for monolithic on-chip nanophotonic architectures,” Photonics Research 7, 437-444, (2019).
[29] D. Benedikovic, L. Virot, G. Aubin, J.-M. Hartmann, F. Amar, B. Szelag, X. Le Roux, C. Alonso-Ramos, P. Crozat, E. Cassan, D. Marris-Morini, C. Baudot, F. Boeuf, J.-M. Fédéli, C. Kopp, and L. Vivien, “Comprehensive Study on Chip-Integrated Germanium Pin Photodetectors for Energy-Efficient Silicon Interconnects,” IEEE Journal of Quantum Electronics 56, Article Sequence Number 8400409, (2020).
[30] J. C. Campbell, "Recent Advances in Avalanche Photodiodes," IEEE Journal of Lightwave Technology 34, 278-285, (2016).
[31] M. Nada, Y. Yamada, and H. Matsuzaki, "Responsivity-Bandwidth Limit of Avalanche Photodiodes: Toward Future Ethernet Systems," IEEE Journal of Selected Topics in Quantum Electronics 24, Article Sequence Number 3800811, (2018).
[32] S. Assefa, F. Xia, and Y. A. Vlasov, "Reinventing germanium avalanche photodetector for nanophotonic on-chip optical interconnects," Nature 464, 80-84, (2010).
[33] Y. Kang, H.-D. Liu, M. J. Paniccia, M. Zadka, S. Litski, G. Sarid, A. Pauchard, Y.-H. Kuo, H.-W. Chen, W. S. Zaoui, J. E. Bowers, A. Beling, D. C. McIntosh, X. Zheng, and J. C. Campbell, "Monolithic germanium/silicon avalanche photodiodes with 340 GHz gain-bandwidth product," Nature Photonics 3, 59-63, (2009).
[34] N. J. D. Martinez, C. T. Derose, R. W. Brock, A. L. Starbuck, A. T. Pomerene, A. L. Lentine, D. C. Trotter, and P. S. Davids, "High-performance waveguide-coupled

Ge-on-Si linear mode avalanche photodetectors," Optics Express 24, 19072-19081, (2016).
[35] L. Virot, P. Crozat, J.-M. Fédéli, J.-M. Hartmann, D. Marris-Morini, E. Cassan, F. Boeuf, and L. Vivien, "Germanium avalanche receiver for low power interconnects," Nature Communications 5, Article number 4957, (2014).
[36] H. T. Chen, J. Verbist, P. Verheyen, P. De Heyn, G. Lepage, J. De Coster, X. Yin, J. Bauwelinck, J. Van Campenhout, and G. Roelkens, "High sensitivity 10Gb/s Si photonic receiver based on a low-voltage waveguide-coupled Ge avalanche photodetector," Optics Express 23, 815-822, (2015).
[37] H. Chen, J. Verbist, P. Verheyen, P. De Heyn, G. Lepage, J. De Coster, P. Absil, B. Moeneclaey, X. Yin, J. Bauwelinck, J. Van Campenhout, and G. Roelkens, "25-Gb/s 1310-nm optical receiver based on a sub-5-V waveguide-coupled germanium avalanche photodiode," IEEE Photonics Journal 7, Article Sequence Number 7902909, (2015).
[38] Z. Huang, C. Li, D. Liang, K. Yu, C. Santori, M. Fiorentino, W. Sorin, S. Palermo, and R. G. Beausoleil, "25 Gbps low-voltage waveguide Si-Ge avalanche photodiode," Optica 3, 793-798, (2016).
[39] X. Zheng, Z. Huang, B. Wang, D. Liang, M. Fiorentino, and R. G. Beausoleil, "Silicon-germanium avalanche photodiodes with direct control of electric field in charge multiplication region," Optica 6, 772-777, (2019).
[40] D. Benedikovic, L. Virot, G. Aubin, J.-M. Hartmann, F. Amar, X. Le Roux, C. Alonso-Ramos, E. Cassan, D. Marris-Morini, P. Crozat, F. Boeuf, J.-M. Fédéli, C. Kopp, B. Szelag, and L. Vivien, "40 Gbps heterostructure germanium avalanche photo receiver on a silicon chip," Optica 7, 775-783, (2020).
[41] D. Benedikovic, L. Virot, G. Aubin, J.-M. Hartmann, F. Amar, X. Le Roux, C. Alonso-Ramos, E. Cassan, D. Marris-Morini, F. Boeuf, J.-M. Fédéli, B. Szelag, and L. Vivien, " Silicon-Germanium Avalanche Receivers With fJ/bit Energy Consumption," IEEE Journal of Selected Topics in Quantum Electronics 28, Article Sequence Number 3802508, (2022).
[42] A. Samani, O. Carpentier, E. El-Fiky, M. Jacques, A. Kumar, Y. Wang, L. Guenin, C. Gamache, P.-C. Koh, and D. V. Plant, "Highly Sensitive, 112 Gb/s O-band Waveguide Coupled Silicon-Germanium Avalanche Photodetectors," in Optical Fiber Communication Conference, Optical Society of America, 2019, p. Th3B.1.
[43] S. Park, Y. Malinge, O. Dosunmu, G. Lovell, S. Slavin, K. Magruder, Y. Kang, and A. Liu, "50-Gbps Receiver Subsystem using Ge/Si Avalanche Photodiode and Integrated Bypass Capacitor," in Optical Fiber Communication Conference, Optical Society of America, 2019, p. M3A.3.
[44] S. A. Srinivasan, J. Lambrecht, M. Berciano, S. Lardenois, P. Absil, J. Bauwelinck, X. Yin, M. Pantouvaki, and J. Van Campenhout, "Highly Sensitive 56 Gbps NRZ O-band BiCMOS-Silicon Photonics Receiver using a Ge/Si Avalanche

Photodiode," in Optical Fiber Communication Conference, Optical Society of America, 2020, p. W4G.7.
[45] S. A. Srinivasan, M. Berciano, P. De Heyn, S. Lardenois, M. Pantouvaki, and J. Van Campenhout, "27 GHz Silicon-Contacted Waveguide-Coupled Ge/Si Avalanche Photodiode," Journal of Lightwave Technology 38, 3044-3050, (2020).
[46] B. Wang, Z. Huang, Y. Yuan, D. Liang, X. Zeng, M. Fiorentino, and R. G. Beausoleil, "64 Gb/s low-voltage waveguide SiGe avalanche photodiodes with distributed Bragg reflectors," Photonics Research 8, 1118-1123, (2020).